Zagazig University Medical Journal
www.zumj.journals.ekb.eg
https://doi.org/10.21608/zumj.2024.292157.3411 Volume 30, Issue 5, August 2024
Manuscript ID ZUMJ-2405-3411 (R2)
DOI /10.21608ZUMJ.2024.292157.3411
Original article

The Possible Role of Hesperidin on Triolein Induced Lung Structural Changes in Adult Male Albino Rats (Histological and Immunohistochemical Study)

Abeer A. Mahmoud*, Samar Abdelaziz Mostafa, Ebtehal Z. Hassan.
Medical Histology and Cell Biology Department, Faculty of Medicine, Zagazig University, Zagazig, Egypt.

***Corresponding author:**
Abeer A. Mahmoud

E -mail:
abeerazeem@hotmail.com

Submit Date 01-06-2024
Revise Date 27-06-2024
Accept Date 28-06-2024

ABSTRACT

Background: Triolein used as a plasticizer, a lubricant, and present in cocoa butter. Its occupational exposure led to health hazards, especially lung injury. Hesperidin antioxidant flavonoid is present in many fruits and vegetables.
The present research aimed to evaluate the possible ameliorative effect of hesperidin on triolein-induced lung structural changes in rats using histological and immunohistochemical study.

Methods: Forty-five adult male albino rats were used. They were divided into Group I: (control group). Group II: rats received 0.2 ml triolein then were sacrificed after 21 days. Group III (triolein and hesperidin): rats subdivided in 2 subgroups: IIIa, IIIb, received triolein as group II and simultaneously received hesperidin 50 mg/kg/day by gavage for 21, 28 days respectively.
Results: Group II showed marked affection of lung tissue. The bronchiolar epithelium showed dark-stained nuclei and vacuolated cytoplasm, desquamated epithelial cells. The alveoli collapsed with thickened interalveolar septa. The interstitial tissue showed congested blood vessels, inflammatory cellular infiltration, and extravasated blood in H&E-stained sections. Group II also showed increased deposition of collagen fibers, increased expression of alpha –Smooth muscle actin (α-SMA) in the interalveolar septa, wall of the blood vessels and bronchioles. Group IIIa, IIIb showed improvements of the previous pathological findings with more improvement in group IIIb
Conclusions: hesperidin could protect the lung from the injurious effect of triolein possibly due to its anti-inflammatory, antioxidant and antifibrotic actions.
Keywords: Lung; Triolein; Hesperidin; Rat.

INTRODUCTION

Triglycerides like triolein are made from oleic acid. It is formed of glycerol and three units of the unsaturated fatty acid. It presents mainly in cocoa butter and olive oil and used in textile industry, an ointment, emulsifiable paste and lotion [1].
Workers are exposed to it through dermal contact at workplace. Also, individuals can be exposed to triolein through different products containing it and by ingestion of its food products [2,3]. It is reported that exposure to triolein induced several structural lung changes and lung fibrosis [4].
Lung fibrosis is a lung damage causes respiratory malfunction with marked dyspnea, disturbance in gas exchange and respiratory failure with poor prognosis with expected survival 2 to 3 years [5].
Its pathogenesis depends mainly on the action of activated fibroblasts and myofibroblasts with excessive accumulation of fibrous tissue and the formation of fibrotic foci [**6**].
Recent research has demonstrated that natural medicine, such as flavonoid active components, can protect against lung injury by reducing oxidative stress and inflammation through the Nrf2-erythroid 2 signaling pathway [7,8].
Flavonoids are naturally occurring phenolic compounds found in fruits, vegetables, and plant roots. They have an antioxidant effect on biological systems. Antioxidant, anti-

inflammatory, antibacterial, anti-mutagenic, and anti-cancer qualities are possessed by flavonoids [9].

Citrus fruits such as lemon, satsuma mandarin, sweet orange, and bitter orange are rich in hesperidin (HES), a flavanone glycoside that is readily available and may be isolated in significant amounts [10].

It is stated that hesperidin inhibits liver fibrosis via decreasing TGF-β1 cytokine which presents in liver and lung fibrosis at high level [11]. It acts as a possible inducer in the transition of epithelium mesenchyme with losing of epithelial cells of cell –cell adhesion and act as mesenchymal stem cells **[**12**].**

Thus, we pointed to assess the role of hesperidin on the lung histological changes caused by triolein treatment in adult male albino rats.

METHODS

I. Chemicals:

- Triolein (powder): was obtained from Sigma-Aldrich.
- Hesperidin (powder): (Sigma Chemical Co., St. Louis, MO, United States of America (USA)) was stored away from direct sunlight at 2–4 ◦C. El Gomhoria, a chemical and medical trading company in Egypt, provided the carboxymethyl-cellulose (vehicle of HES).

II. Experimental animals

Forty-Five adult male albino rats weighing between 200 and 250 grams were used in the study. They were from breading animal home, Faculty of Medicine, Zagazig University. The experimental protocol was approved by Zagazig University's research ethics committee. Approval number: ZU-IACUC/3/F/ 1 2 8/2022. Throughout the experiment, the rats were housed at a controlled temperature (23±1 °C) and humidity (55±5%), with regular cycles of light and dark and unrestricted access to food and drink.

III. Experimental design

The animals were divided into three groups as follows:

Group I (control group): 15 rats were subdivided into three subgroups, 5 animals each.

Ia: rats left without being given medical treatment.

Ib: A caudal vein injection of 0.2 ml saline (the triolein vehicle) was administered.

Ic: rats were given hesperidin 50 mg/kg/day dissolved in 1% carboxymethyl-cellulose (CMC) by gavage for 28 days.

Group II (triolein treated group): 10 rats each rat was injected 0.2 ml of triolein in the caudal vein daily for 21 days [3].

Group III (triolein and hesperidin treated group): 20 rats subdivided in 2 subgroups:

IIIa: 10 rats received triolein as group II, from the first day of injection, each rat was given hesperidin 50 mg/kg/day dissolved in 1% carboxymethyl-cellulose (CMC) via gavage for 21 days [13].

IIIb: 10 rats received triolein as group II, from the first day of injection, each rat received hesperidin 50 mg/kg/day by gavage for 28 days [14].

III. Methods

After the last dose, animals from all groups were fasted overnight then they were anaesthetized with an intraperitoneal injection of 75 mg/ kg ketamine [15]. The chest was opened and specimens of the left lung of each rat of all groups underwent procedures such as immunohistochemical staining for alpha-smooth muscle actin (α-SMA), hematoxylin and eosin staining, and electron microscopy examination.

Light microscope technique:

For light microscopy, following a 10% neutral-buffered formalin immersion, the specimens underwent washing, dehydration, clearing, and paraffin embedding. 5 µm thick sections were stained using:

- H&E [16].
- Mallory's trichrome to determine the extent of lung fibrosis **[**16**]**.

- Immunohistochemical expression for α-SMA: 1ry antibody: Monoclonal Mouse IgG2A, Catalog # MAB1420(14). PBS was used to dewax, rehydrate, and clean sections that were 5 µm thick. Next, during the full night at 4°C in a humid atmosphere, the sections were incubated with the primary antibody. The sections were incubated with the corresponding biotinylated secondary antibody for an hour at room temperature following three PBS rinses. Following a ten-minute addition of streptavidin peroxidase, the samples underwent three additional PBS washes. Immunoreactivity was shown using 3,3′-diaminobenzidine-hydrogen peroxide as a chromogen. The sections were counterstained with Mayer's hematoxylin. Primary antibodies were not used in the preparation of the negative control sections [17]. Olympus microscopes (C5060-AUD, 5H01155 JAPAN) were used to see the sections, and digital cameras (Canon PowerShot A620, England, UK) were used to take pictures. The photomicrographs were enhanced with a scale bar in accordance with calibration.

Transmission electron microscope technique:

The specimens were fixed in 2% buffered glutaraldehyde, washed in PBS, fixed in 1% osmium tetroxide, dehydrated in alcohol, and embedded in epoxy resins for transmission electron microscopy. Under a light microscope, semithin sections (1 µm thick) were prepared and stained with 1% toluidine blue, while ultrathin sections (70-90 nm) were stained with lead citrate and uranyl acetate [18]. The ultrathin sections were examined and photographed using a JEOL JEM 2100 EXII electron microscope (Jeol Ltd), Electron Microscope Research Laboratory, Faculty of Agricultural, Mansoura University, Egypt.

IV. **Morphometric study**:

At Cairo University's Faculty of Dentistry, image analysis was carried out in the pathology department's lab. Leica Microsystems Imaging Solution, Ltd., Cambridge, UK, made the Leica Qwin 500 image analyzer computer system that they used [19]. With five distinct slices from five separate rats in each group, this was done in five non-overlapping fields at a 400x magnification.

To do a quantitative evaluation, the following parameters were calculated:

1. The thickness of interalveolar septum in H&E-stained sections
2. Area % of collagen fiber content (in Mallory's trichrome-stained sections).
3. Area % of immunohistochemical reaction for α-SMA among the different studied groups.

STATISTICAL ANALYSIS:

A statistical analysis was performed on the area percentage of α-SMA immunohistochemical reactivity and Mallory's trichrome-stained sections for each of the study groups. The interalveolar septal thickness was measured in the H&E-stained sections. Each experiment's result was displayed as mean ± SD (standard deviation). One-way analysis of variance (ANOVA) was used to evaluate the group differences, followed by the Post hoc least significant difference (LSD) test. In every comparison, a difference considered significant was defined as $P<0.05$. Every analysis was performed using IBM SPSS 19.0 [20].

Histological RESULTS:

Light microscopic results:

The control group's lung sections stained with Hematoxylin and Eosin (H&E) showed the typical architecture of rounded or polygonal alveoli, alveolar sacs, and bronchioles. Blood vessels were located within the narrow interalveolar septa that divided the alveoli (**Figure 1A**).

The group treated with triolein showed pronounced lung tissue affection. In the bronchiolar lumen, dark-stained nuclei and vacuolated cytoplasm were present in the bronchiolar epithelium along with desquamated epithelial cells. Alveoli collapsed and the interalveolar septa thickened. Congested blood vessels, inflammatory cell infiltration, and extravasated blood were observed in certain regions of the interstitial tissue (**Figure 1B**).

The hesperidin and triolein subgroup IIIa displayed localized regions of collapsed alveoli divided by thick interalveolar septa. Epithelium with darkly stained nuclei lined the bronchioles. The interalveolar septa showed evidence of extravasated blood and congested blood vessels (**Figure 1C**).

There were a few congested blood vessels together with thin interalveolar septa separating obviously normal alveoli and alveolar sacs in hesperidin and triolein subgroup IIIb (**Figure 1D**).

Mallory's trichrome stain:

Few collagen fibers with blue discoloration were seen in the walls of bronchioles, surrounding blood vessels, and in the interalveolar septa in sections of the control lung stained with Mallory trichrome (**Figure 2A**). In contrast, the triolein-treated group's bronchiole wall, surrounding blood vessels, and interstitium between alveoli all showed noticeably higher levels of collagen fibers (**Figure 2B**). Nonetheless, the collagen fibers rose in the triolein and hesperidin subgroup IIIa (**Figure 2C**). Collagen fibers were seen in significant amounts in the area around blood capillaries, in the bronchiole wall, and in the space between alveoli in hesperidin and triolein subgroup IIIb (**Figure 2D**).

Immunohistochemical staining of α-SMA:

A slight positive reaction was observed in the interalveolar septa of the control group when using the immunoperoxidase technique to measure the α-SMA immunoreaction (**Figure 3A**). The triolein -treated group showed intense positive immune expression of α-SMA in the form of brown coloration in the interalveolar septa, wall of the blood vessels and bronchioles (**Figure 3B**). However, triolein and hesperidin subgroup IIIa revealed moderate positive immune reaction in the interalveolar septa (**Figure 3C**). Conversely, the interalveolar septa of the hesperidin and triolein subgroup IIIb displayed minimal positive immunological expression of α-SMA (**Figure 3D**).

Transmission electron microscopic results:

Ultrathin sections of the control lung revealed the blood air barrier, which is made up of type I pneumocyte processes, fused basal laminae of pneumocyte type I, and endothelial cell cytoplasm (**Figure 4A**).

The group treated with triolein displayed thick and wrinkled blood air barriers, indicating severely damaged lung tissue (**Figure 4B**).

Focal thickening of the blood air barriers was observed in the triolein and hesperidin subgroup IIIa (**Figure 4 C**).

The blood air barrier, which is made up of type I pneumocyte processes, blood endothelium basal laminae, and endothelial cell cytoplasm, improved in hesperidin and triolein subgroup IIIb (**Figure 4D**).

The control group's type II pneumocytes were observed to have euchromatic nuclei with peripheral heterochromatin. They had mitochondria and lamellar bodies in their cytoplasm and microvilli observed on their surfaces. Type I pneumocytes were found to have elongated nuclei (**Figure 5A**).

The group treated with triolein had lung tissue affection as evidenced by an increase in collagen fibers in the interstitium. The nuclear envelope of type II pneumocytes was seen irregular. They had destroyed microvilli on their surfaces and lamellar bodies with electron-dense material and vacuoles in their cytoplasm (**Figure 5B**).

Other sections displayed mitochondria with irregular cristae, vacuoles, and heterochromatic nuclei characteristic of pneumocyte type II (Figure 5c). In electron micrographs of the same group, alveolar macrophages were also seen, and their nuclei showed peripheral heterochromatin. Lysosomes and electron-dense bodies were present in their cytoplasm (**Figure 5D**).

Triolein and hesperidin subgroup IIIa revealed pneumocyte type II with surface microvilli, nuclei with peripheral heterochromatin, mitochondria with abnormal cristae and numerous lamellar bodies containing electron-dense material (Figure5e). Other sections showed thick interstitium contained collagen fibers (Figure5f). Alveolar macrophages with indented nuclei and electron-dense bodies were also detected **(Figure 5G**). Triolein and hesperidin subgroup IIIb showed interstitium with few collagen fibers. Pneumocyte type II detected with nuclei contained peripheral heterochromatin and apparently normal lamellar bodies and mitochondria in their cytoplasm. Microvilli were seen on their surfaces (**Figure 5h**).

Morphometric and statistical analysis results:

- Group II exhibited a highly statistically significant rise in mean septal thickness of the lung alveoli when compared to the control group, while group IIIb show a highly statistically significant decrease when compared to group II (**Table 1 & Figure 6**).
- Group II showed a highly statistically significant increase in the mean area percentage of collagen fibers in lung sections compared to the control group, while groups IIIa and IIIb showed a highly statistically significant decrease in contrast to group II (**Table 1 & Figure 6**).
- The mean area% α-SMA immune reaction revealed a highly statistically significant difference between the various groups under study; group II showed a highly statistically significant increase when compared to the control group, and groups IIIa and IIIb showed a highly statistically significant decrease when compared to group II (**Table 1 & figure 6**).

Table (1): Comparison between different studied groups regarding the mean septal thickness, area % of collagen fibers, and area % of α- SMA using ONE WAY ANOVA:

	Group I (Control group)	Group II (Triolein treated group)	Group IIIa (Triolein + hesperidin group	Group IIIb (Triolein + hesperidin group	F-value	P-value
Septal thickness In nm	0.8±0.32	22.09± 7.78	11.3± 3.38	2.15±1.89	51.284	<0.000001 *
Area % of collagen fibers	6.45 ± 3.32	33.8 ± 6.52	17.2 ± 5.9	9.7 ± 5.07	51.914	<0.000001 *
Area % of α- SMA	1.27 ± 0.64	7.85 ± 2.78	5.5 ± 2.64	3.01 ± 1.46	19.0674	<0.000001 *

*Highly significant difference

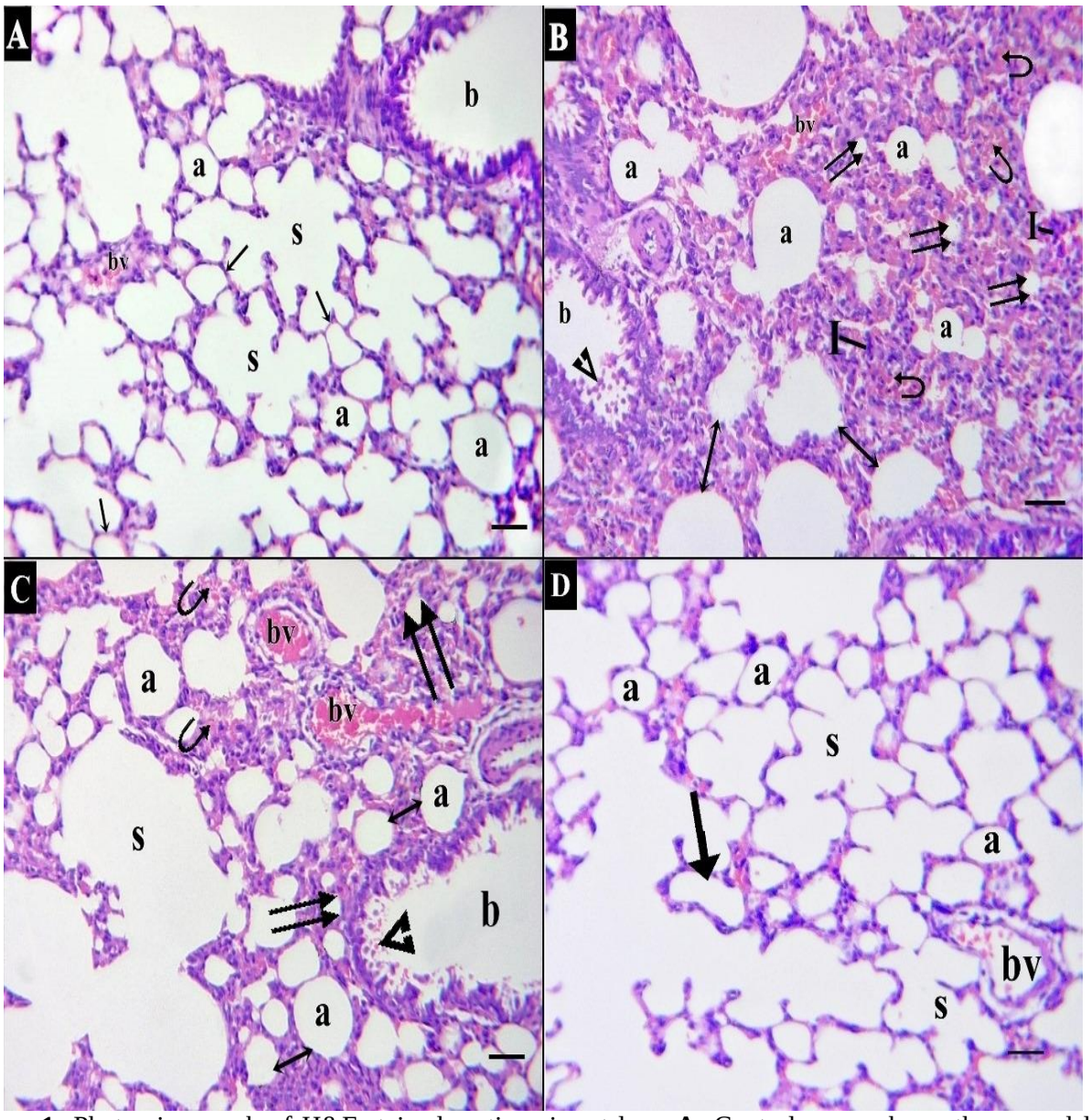

Figure 1: Photomicrograph of H&E-stained sections in rat lung **A:** Control group shows the normal lung histological structure; bronchioles (b), polygonal alveoli (a) that are separated by thin interalveolar septa (arrows), alveolar sacs (s), and the interstitium with blood vessels (bv). **B:** Triolein treated group reveals marked affection of bronchiole (b), that is showing desquamated epithelial cells (arrowhead) in its lumen. Collapsed alveoli (double arrows) with thickened interalveolar septa (double headed arrow), congested blood vessels (bv), extravasated blood (curved arrow) and interstitial inflammatory cellular infiltration (I) are also seen. **C:** Triolein and hesperidin subgroup IIIa: shows alveoli (a), alveolar sacs (s) and bronchioles (b) with desquamated epithelial cells (arrowhead) in the lumen. Some alveoli are collapsed (double arrow). The interalveolar septa (double headed arrow) are thick. Extravasated blood (curved arrow) and congested blood vessels (bv) are noticed in the interstitium. **D:** Triolein and hesperidin subgroup IIIb: shows normal alveoli (a) and alveolar sacs (s) are separated by thin interalveolar septa (arrow). Few congested blood vessels (bv) are also noticed.

(H&E X 200, scale bar 30 µm)

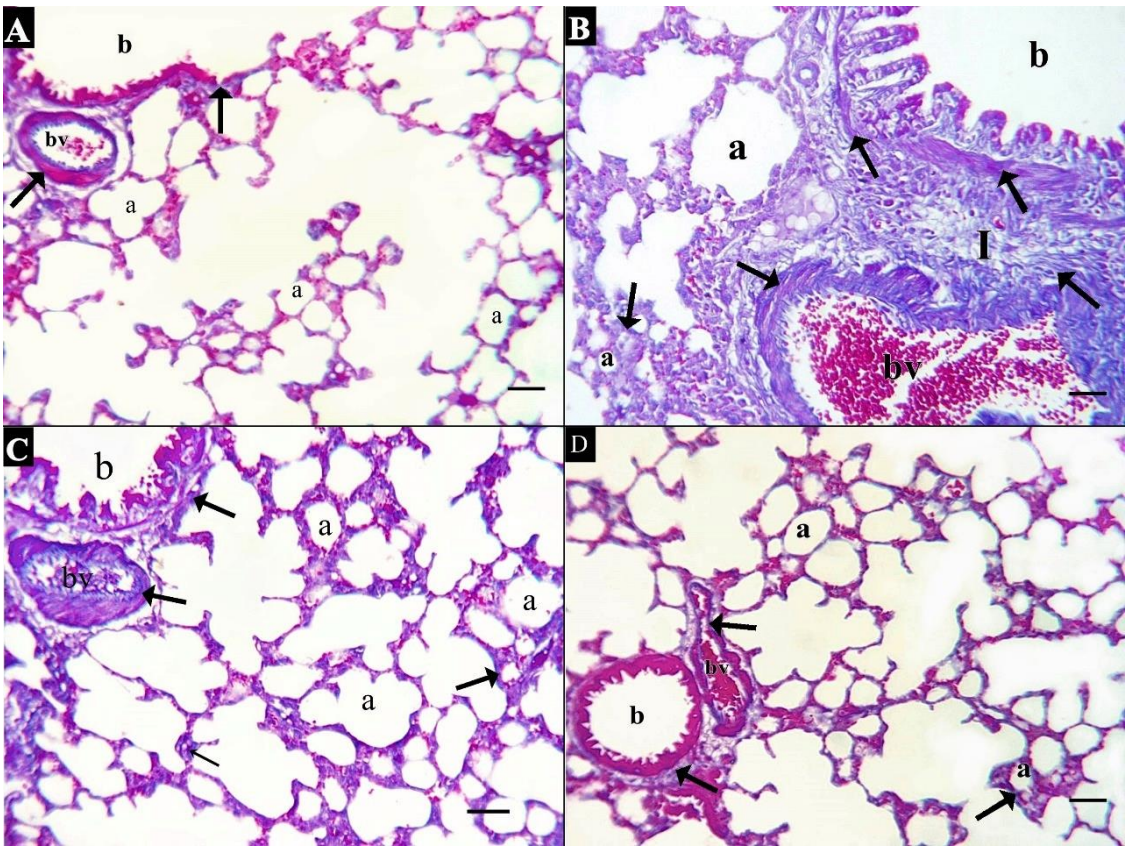

Figure 2: Photomicrograph of Mallory trichrome–stained sections **A:** control lung showing minimal collagen fibers (arrows) around blood vessel (bv), in the interalveolar septa and wall of bronchiole (b). **B:** Triolein treated group showing increased collagen fibers (arrows) in the interstitium (I) between alveoli, around blood vessel (bv) and wall of bronchiole (b). **C:** Triolein and hesperidin subgroup IIIa reveals some collagen fibers in interstitium, around blood vessel (bv) and wall of bronchiole(b). **D:** Triolein and hesperidin subgroup IIIb: shows few collagen fibers (arrows) are detected in interstitium, around blood vessel (bv) and wall of bronchiole(b).
(Mallory trichrome × 200, scale bar 30 µm)

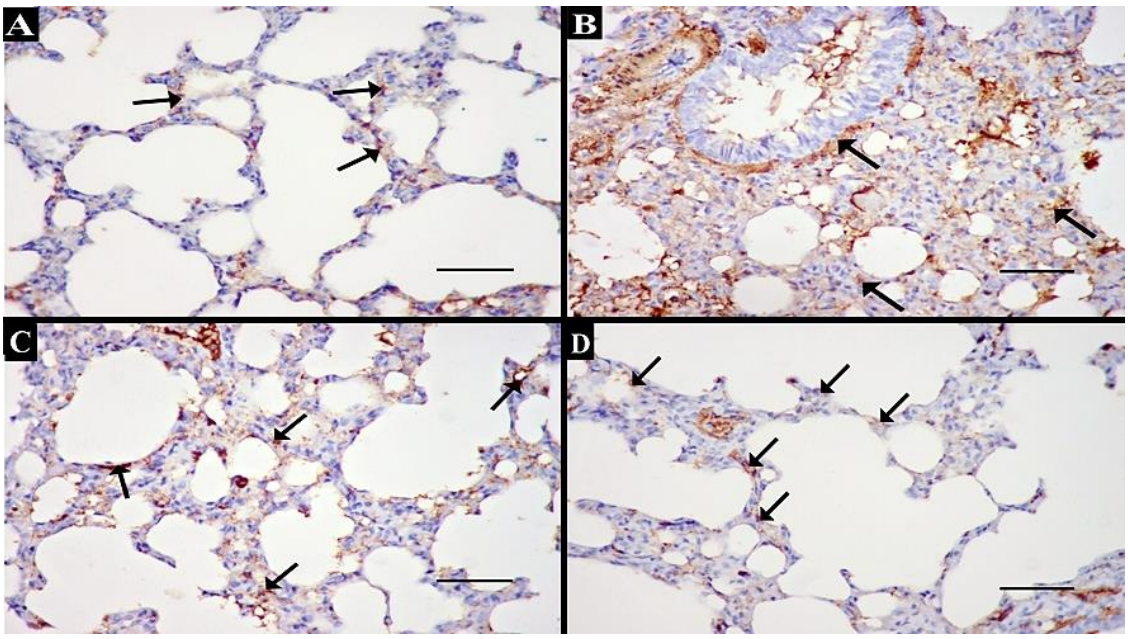

Figure 3: Photomicrograph of α-smooth muscle actin–stained sections **A:** control group shows faint positive reaction in the interalveolar septa (arrows). **B:** Triolein -treated group reveals intense expression of α-SMA (arrows) in the interalveolar septa and wall of bronchiole. **C:** Triolein and hesperidin subgroup IIIa reveals

a moderate reaction (arrows) in the interalveolar septa. **D:** Triolein and hesperidin subgroup IIIb shows few reactions in the interalveolar septa (arrows).
(α-SMA × 400, scale bar 30 µm)

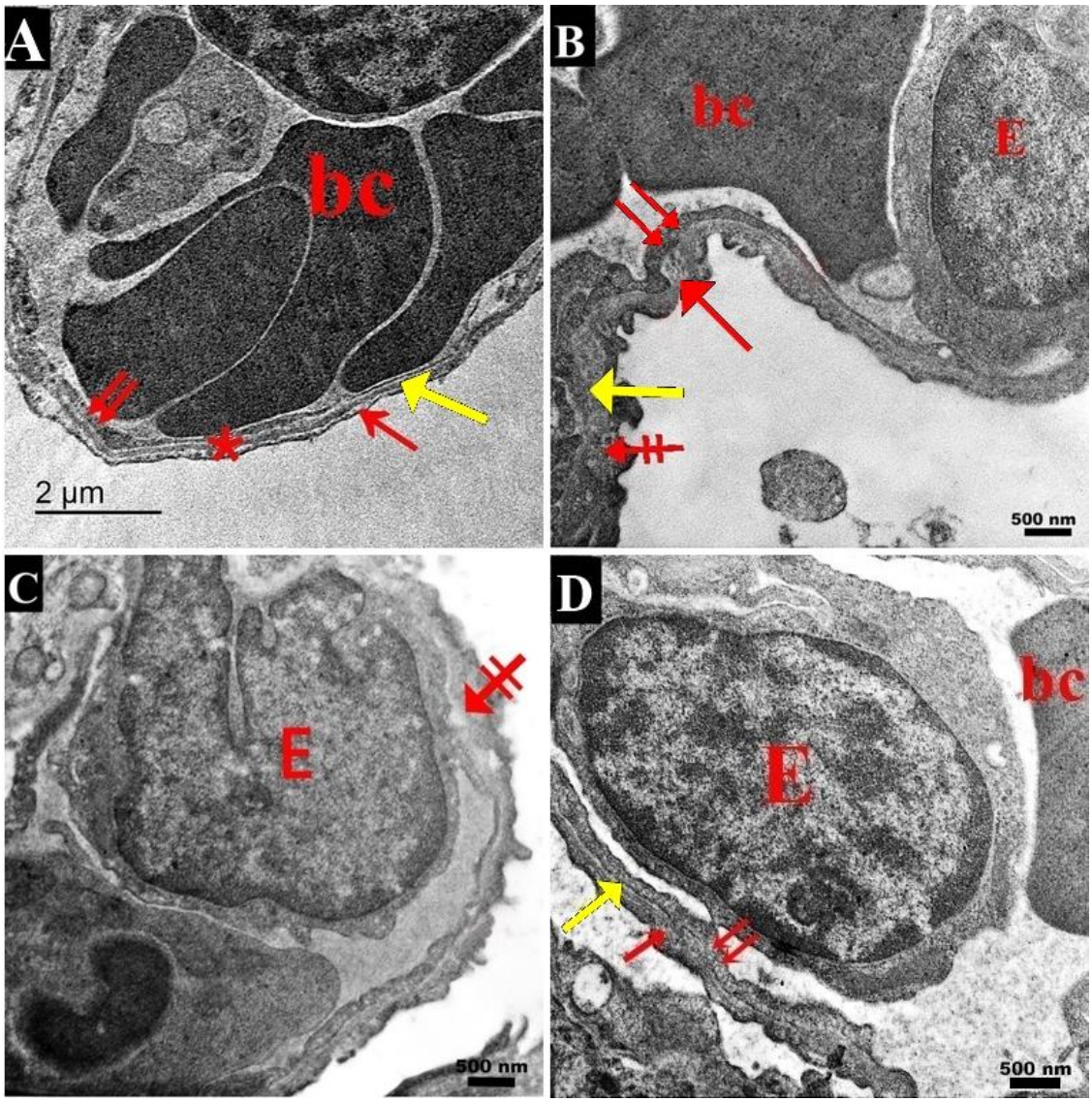

Figure 4: Transmission electron micrograph of the lung tissue of rats. **A:** control group shows the regular blood air barrier (asterisk) that is formed of type I pneumocyte processes (red arrow), fused basal laminae of pneumocyte type I and blood endothelium (yellow arrow) and endothelial cell cytoplasm (double arrow). **B:** Triolein-treated group reveals thickened and wrinkled (crossed arrow) blood air barrier that is formed of endothelium (double arrow), fused basal lamina (yellow arrow) and pneumocyte type I process (red arrow). Endothelial cell (E) of blood capillary is also seen. **C:** Triolein and hesperidin subgroup IIIa, displays focal thickening of blood air barrier (crossed arrow). **(D):** Triolein and hesperidin subgroup IIIb shows normal blood air barrier with intact type I pneumocyte processes (red arrow), fused basal lamina (yellow arrow) and endothelium (double arrow). Endothelial cell (E) is also noticed.
(TEM; scale bar A: 2 µm, B: 500 nm, C: 500 nm and D: 500 nm)

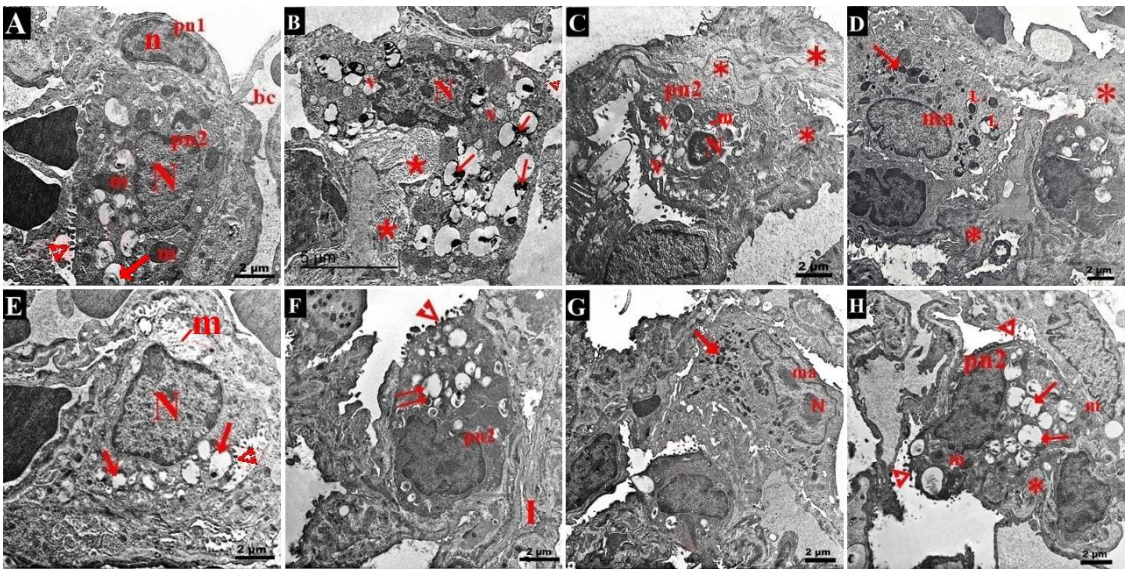

Figure 5: Transmission electron micrograph of the control group **(A):** shows Pneumocyte type II (pn2) with euchromatic nucleus (N) and peripheral heterochromatin. The cytoplasm has lamellar bodies (arrow) and mitochondria (m). Microvilli (arrowhead) are seen on its surface. Pneumocyte type I (pn1) is also noticed with elongated nucleus (n). **B:** Triolein-treated group reveals pneumocyte type II nucleus (N) with irregular nuclear envelope. Lamellar bodies (arrow) with electron-dense material and vacuoles (v) are observed in the cytoplasm. Excessive amount of collagen fibers (asterisk) in the interstitium and destructed microvilli (arrowhead) on the surface are detected. **C:** Triolein-treated group shows pneumocyte type II with heterochromatic nucleus (N), vacuoles (v) and mitochondria (m) with destructed cristae. Collagen fibers (asterisk) are also noticed in the interstitium. **D:** Alveolar macrophage is observed in Triolein- group with nucleus (N) contained peripheral heterochromatin. Lysosomes (L) and electron-dense bodies (arrow) are seen in the cytoplasm. Collagen fibers (asterisk) are also seen. **E:** Triolein and hesperidin subgroup IIIa exhibits pneumocyte type II with nucleus (N) contained peripheral heterochromatin, surface microvilli (arrowhead), mitochondria (m) with abnormal cristae and numerous lamellar bodies (arrow) containing electron-dense material. **F:** Other sections of the same group show thick interstitium (I) with collagen fibers. Pneumocyte type II (pn2) is also observed with lamellar bodies (double arrow) and microvilli (arrowhead). **G:** Alveolar macrophage (ma) in Triolein and hesperidin subgroup IIIa appears with indented nucleus (N) and electron-dense bodies (arrow) in its cytoplasm. **H:** Triolein and hesperidin subgroup IIIb displays few collagen fibers (asterisk) in interstitium. Pneumocyte type II (pn2) is observed with nucleus contained peripheral heterochromatin and apparently normal lamellar bodies (arrow) and mitochondria (m) in the cytoplasm. Microvilli (arrowhead) are noticed on the surface.
(TEM; scale bar A: 2 µm, B: 5 µm, C, D, E, F, G, H: 2 µm)

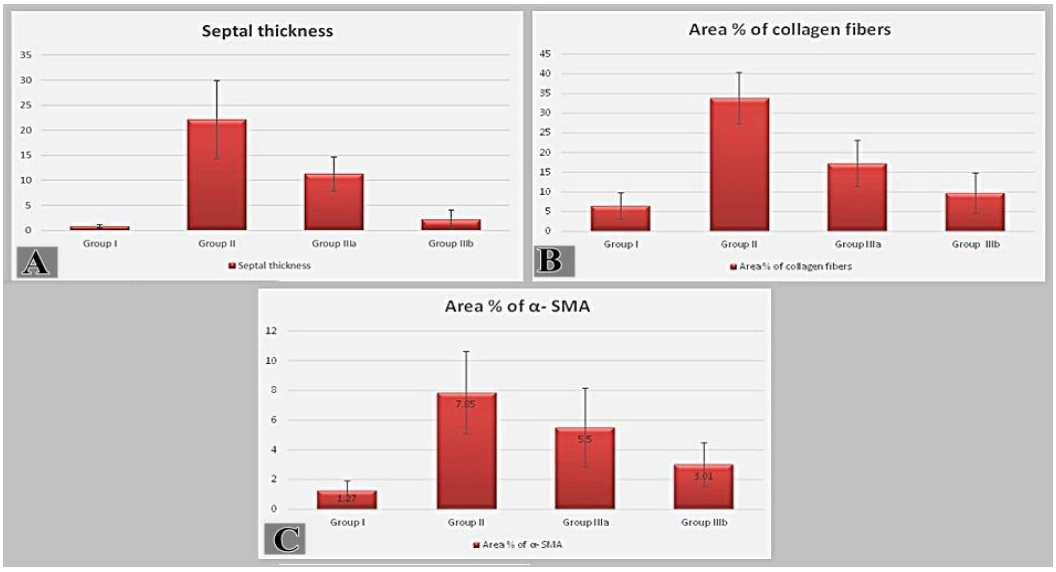

Figure 6: Comparison between different studied groups regarding the mean septal thickness, the mean Area % of collagen fibers, and the mean Area % of α- SMA.

DISCUSSION:

This work aimed to clarify any possible changes in the lung histological structure of adult male albino rats exposed to triolein and explore the ameliorative role of hesperidin.

In this study, examination of H&E-stained sections of triolein- treated group revealed bronchiolar epithelial cells with desquamated epithelial lining, vacuolated cytoplasm, and darkly stained nuclei. Additionally, thicker interalveolar septa were observed in between the alveoli. There was a noticeable infiltration of inflammatory cells and congested blood vessels in the interstitium.

Numerous studies indicate that the oxido-inflammatory state that triolein induces includes the production of reactive oxygen species (ROS) and reactive nitrogen species, enhanced alveocapillary permeability, intra-alveolar and interstitial fluid accumulation, polymorphonuclear leukocyte infiltration, activation of oxidant enzymes, cytokine secretion, and adhesion molecule production [21].

In H&E-stained sections of the triolein group, congested blood vessels were visible due to triolein's increased lung angiotensin II (Ang II) [22]. Furthermore, increased tissue exudate invasions by cells show that angiotensin II increases the permeability of blood vessels, which has more pro-inflammatory and pro-fibrotic effects [23].

In the current work, the triolein-treated group had increased collagen fibers around bronchioles, blood vessels, and in between alveoli that was statistically confirmed by a highly significant increase in the area percent of collagen fibers in comparison to the control. According to Yamada et al. [24] triolein induces an inflammatory response that results in the accumulation of collagen fibers in the interalveolar septa and the release of pro-fibrotic mediators from mast cells and pro-fibrotic mediators from macrophages. This process can account for the significantly elevated collagen levels.

The elevated α-SMA expression in the triolein-treated group in our study was attributed by Marcel et al. [25] to the major actin isoform, α-SMA, which is essential for fibrogenesis and found in myofibroblasts. They added that myofibroblasts, fibroblasts with a distinct shape and metabolism that express alpha-SMA, are key players in the development of the fibrotic response. When fibroblasts with higher α-SMA expression mature into myofibroblasts, transforming growth factor-beta (TGF-) is formed more frequently when a person consumes triolein.

Ultrastructurally, the triolein treated group showed thick and wrinkly blood air barriers, type II pneumocytes with damaged microvilli on their surface, and lamellar bodies containing electron-dense material and vacuoles in their cytoplasm. Triolein is claimed by Kandhare et al. [26] to trigger the release of pulmonary lipase, which in turn hydrolyzes it into hazardous free fatty acids. This process activates peripheral mast cells to create renin and attracts macrophages, so stimulating the release of inflammatory mediators. Pro-inflammatory cytokines, such as interleukins (ILs) and tumor necrosis factor (TNF-), have been linked to an increase in reactive oxygen species (ROS) input. This results in death of the alveolar epithelial cells and denudation of the basement membrane, which speeds up the epithelial cells' transition into mesenchyme and the pulmonary architectural remodeling.

H&E-stained sections of **triolein and hesperidin** treated subgroups **(IIIa, IIIb) for 21, 28 days showed progressive recovery in the histological structure of the lung tissue which is duration dependent.** It works by scavenging free radicals and by preserving intracellular levels of glutathione and superoxide dismutase (SOD), avoiding lipid peroxidation and tissue damage [27, 28].

Consistent with our findings, Li et al. (29) documented that flavonoid could impact learning and memory role by preventing extreme apoptosis and oxidative stress in ALCL3-exposed rats. Furthermore, Muhammad et al. (30) reported that Hesperidin rescued lipopolysaccharide (LPS)-induced neuronal apoptosis by reducing the expression of associated X protein (BAX) and caspase-3 protein and promoting the Bcl-2 protein level.

In our study, triolein and hesperidin treated subgroups (IIIa, IIIb) for 21, 28 days displayed a reduction in the amount of collagen fibers surrounding blood capillaries, in the bronchiole wall, and in the space between alveoli. There was a non-significant difference in the area % of collagen fibers in comparison to the control group. Hesperidin was reported to improve pulmonary edema and lung shape by reducing the deposition of collagen fibers in the space between alveoli and surrounding blood vessels, modify the expression of pro-inflammatory cytokines and chemokines, and reduce the production of

polymorphonuclear neutrophils and macrophages in the airways [31]. Further findings revealed that hesperidin inhibits the TGF-/Smad3 signaling pathway, reducing collagen-1 production by inhibiting TGF-/Smad3 signaling [32].

Also, hesperidin dramatically reduced in vivo oxidative DNA damage with antiapoptotic potential. Additionally, it considerably preserves the integrity of the alveolar membrane, and prevents mast cell infiltration [33,34].

Declaration of interest and Funding information: The authors declare no conflict of interest to disclose.

Conclusion:

The histological structure of the lungs in adult albino rats is negatively impacted by triolein. Our research indicates that the use of hesperidin plays duration-dependent protective and anti-fibrotic activities that counteract the deleterious effects of triolein. Triolein should therefore be used with caution and, if necessary, with great care.

REFERENCES:

1-McIff TE, Poisner AM, Herndon B, Lankachandra K, Molteni A, Adler F. Mitigating effects of captopril and losartan on lung histopathology in a rat model of fat embolism. J Trauma Acute Care Surg2011; 70(5) :1186-91. https://doi.org/10.1097/TA.0b013e3181e50df6

2-kandeel S and Estfanous R. The Possible Protective Effect of Magnolol on Triolein-Induced Lung Structural Changes in Rats: Histological and Immunohistochemical Study. Egyptian J of histology 2022;45(2):359-71. DOI: 10.21608/EJH.2021.62560.1429

3-Poisner AM, Adler F, Uhal B, McIff TE, Schroeppel JP, Mehrer A. Persistent and progressive pulmonary fibrotic changes in a model of fat embolism. J. Trauma Acute Care Surg2012;72(4) 992-98. DOI: 10.1097/TA.0b013e31823c96b0.

4-David F, Medvedovici A, Sandra P. Oils, Fats and Waxes: Supercritical Fluid Chromatography. 1st ed., Academic Press, Cambridge (Massachusetts). Elsevier. 2000:3567-75.

5-King TE, Pardo A, Selman M. Idiopathic Pulmonary Fibrosis. The Lancet2011; 378 (9807): 1949–61. PMID: 21719092. DOI: 10.1016/S0140-6736(11)60052-4.

6-Selman M, Pardo A. The epithelial/fibroblastic pathway in the pathogenesis of idiopathic pulmonary fibrosis. Am J Respir Cell Mol Biol 2003;29(3):93-7. PMID: 14503564.

7-Liang W, Greven J, Fragoulis A, Horst K, Bläsius F, Wruck C, et al. Sulforaphane dependent up-regulation of NRF2 activity alleviates both systemic inflammatory response and lung injury after hemorrhagic shock/resuscitation in mice. Shock Inj. Inflamm. Sepsis Lab. Clin. Approaches 2022, 57, 221–229. doi: 10.1097/SHK.0000000000001859. PMID: 34559743.

8-Luan R, Ding D, Yang J. The protective effect of natural medicines against excessive inflammation and oxidative stress in acute lung injury by regulating the Nrf2 signaling pathway. Front. Pharmacol. 2022, 13, 1039022. doi.org/10.3389/fphar.2022.1039022

9- Li X, Hu X, Wang J, Xu W, Yi C, Ma R, Jiang H. Inhibition of autophagy via activation of PI3K/Akt/mTOR pathway contributes to the protection of hesperidin against myocardial ischemia/reperfusion injury. Int. J. Mol. Med. 2018, 42, 1917–1924. doi: 10.3892/ijmm.2018.3794

10- Kandemir FM, Kucukler S, Eldutar E, Caglayan C, Gülçin I. Chrysin protects rat kidney from paracetamol-induced oxidative stress, inflammation, apoptosis, and autophagy: A multi-biomarker approach. Sci. Pharm. 2017, 85, 4. doi: 10.3390/scipharm85010004. PMID: 28134775; PMCID: PMC5388142.

11-Lin X, Kong LN, Huang C, Ma TT, Meng XM, He Y, et al. Hesperetin derivative-7 inhibits PDGF-BB- induced hepatic stellate cell activation and proliferation by targeting Wnt/β-catenin pathway. Int Immunopharmacol2015;25(2):311-20. DOI: 10.1016/j.intimp.2015.02.009

12-Gao R, Chen R, Cao Y, Wang Y, Song K, Zhang Y, et al. Emodin suppresses TGF-β1-induced epithelial-mesenchymal transition in alveolar epithelial cells through Notch signaling pathway. Toxicol Appl Pharmacol. 2017; 318:1-7. doi: 10.1016/j.taap.2016.12.009.

13- Görmeli CA, Saraç K, Çiftçi O, Necati Timurkaan N, Malkoç S. The effects of hesperidin on idiopathic pulmonary fibrosis evaluated by histopathologial-biochemical and micro-computed tomography examinations in a bleomycin-rat model Biomedical Research 2016; 27 (3): 730-35.

14- Shehata AS, Mohamed DA, Hagras SM, El-Beah SM, Elnegris HM. The role of hesperidin in ameliorating retinal changes in rats with experimentally induced type 1 diabetes mellitus and the active role of vascular endothelial growth factor and glial fibrillary acidic protein. Anat Cell Biol 2021;54(4):465-78. doi: 10.5115/acb.21.105. PMID: 34936987; PMCID: PMC8693142.

15- El Bana E, Shawky L (2019) The appropriate time for stem cell transplantation in albino rat with amiodarone induced lung fbrosis: histological and immunohistochemical study. Egypt J Histol 42(1):121–32. DOI: 10.21608/EJH.2018.4675.1017

16-Bancroft JD, Gamble M. Theory and practice of histological techniques. 6th ed. Philadelphia: Churchill Livingstone. Elsevier Health Science 2008; 126–27.

17-Ramos-Vara J, Kiupel M, Baszler T, Bliven L, Brodersen B. et al. Suggested guidelines for immunohistochemical techniques in veterinary diagnostic laboratories. J Vet Diagn Invest 2008; 20:393-413. DOI: 10.1177/104063870802000401

18-Hayat M. Principles and Techniques of Electron Microscopy Biological Applications. 4th ed., Macmillan Press, Scientific Medical LTD. London2000;230-44. DOI:10.1006/anbo.2001.1367

19-Jensen E. Quantitative Analysis of Histological Staining and Fluorescence Using Image J Anat2013;296(12):378-81. DOI: 10.1002/ar.22641

20- Dawson-Saunders B and Trapp R. Basic and clinical biostatics. 3rd ed. New York. Lang Medical Book, McGrow Hill Medical Publishing Division2001;161–218

21- Golbidi S, Moriuchi H, Yang C, Irikura M, Irie T, Hamasaki N. Preventive effect of phosphoenolpyruvate on hypoxemia induced by oleic acid in Guinea pigs. Biol Pharm Bull 2003;26(3):336-40. doi: 10.1248/bpb.26.336. PMID: 12612443.

22- Chang H, Chang CY, Lee HJ, Chou CY, Chou TC. Magnolol ameliorates pneumonectomy and monocrotaline-induced pulmonary arterial hypertension in rats through inhibition of angiotensin II and endothelin-1 expression. Phytomed 2018;51: 205-13. PMID: 30466619 DOI: 10.1016/j.phymed.2018.10.001

23-Kim HJ, Kim YW, Lee IS, Song JW, Jeong YJ, Choi SH. Intra-arterial delivery of triolein emulsion increases vascular permeability in skeletal muscles of rabbits. Acta Vet. Scand 2009; 51(1) 1-7. doi: 10.1186/1751-0147-51-30

24- Yamada M, Kurihara H, Kinoshita K, Sakai T. Temporal expression of alpha-smooth muscle actin and drebrin in septal interstitial cells during alveolar maturation. J. Histochem. Cytochem2005;53(6) :735-44. DOI: 10.1369/jhc.4A6483.2005

25- Marcel J, Federico A, Alan P, Tim Q, Kamani L etal. Long-term Effects of Triolein on the Pulmonary Clara Cells in a Rat Model for Fat Embolism Syndrome. CHEST Journal 2010; 138(4), 227A DOI:https://doi.org/10.1378/chest.10659

26- Kandhare AD, Bodhankar SL, Mohan V, Thakurdesai PA. Effect of glycosides based standardized fenugreek seed extract in bleomycin-induced pulmonary fibrosis in rats: Decisive role of Bax, Nrf2, NF-κB, Muc5ac, TNF-α and IL-1β. Chem Biol Interact 2015; 25(237):151-65. doi: 10.1016/j.cbi.2015.06.019. Epub 2015 17. PMID: 26093215.

27- Haddadi GH, Rezaeyan A, Mosleh-Shirazi MA, Hosseinzadeh M, Fardid R, Najafi M et al. Hesperidin as Radioprotector against Radiation-induced Lung Damage in Rat: A Histopathological Study. J Med Phys2017;42(1):25-32. doi: 10.4103/jmp.JMP_119_16

28-Rezaeyan A, Fardid R, Haddadi GH, Takhshid MA, Hosseinzadeh M, Najafi M, et al. Evaluating radioprotective effect of hesperidin on acute radiation damage in the lung tissue of rats. J Biomed Phys Eng 2016; 6:165–174. PMID: 27853724 PMCID: PMC5106549

29- Li S, Zhang Q, Ding Y, Wang X, Liu P. Flavonoids ameliorate aluminum chloride-induced learning and memory impairments via suppression of apoptosis and oxidative stress in rats. J Inorg Biochem 2020; 212. doi: 10.1016/j.jinorgbio.2020.111252.

30- Muhammad T, Ikram M, Ullah R, Rehman SU, Kim MO. Hesperedin, a citrus flavonoid, attenuates LPS-induced neuroinflammation, apoptosis and memory impairments by modulating TLR4/NF-κB signaling. Nutrients 2019; 11(3):648. doi: 10.3390/nu11030648. PMID: 30884890; PMCID: PMC6471991.

31- Wu FR, Jiang L, He XL, Zhu PL, Li J. Effect of hesperidin on TGF-beta1/Smad signaling pathway in HSC. Zhongguo Zhong Yao Za Zhi 2015; 40:2639–2643. PMID: 26697692

32- Yeh CC, Kao SJ, Lin CC, Wang SD, Liu CJ, Kao ST. The immunomodulation of endotoxin-induced acute lung injury by hesperidin in vivo and in vitro. Life Sci 2007; 80:1821–1831. DOI: 10.1016/j.lfs.2007.01.052.

33- Yu H-b, Li L, Ren Z-x, Shen J-l, Sudha NB, Raju AB, et al. Inhibition of hesperidin on epithelial to mesenchymal transition of non-small cell lung cancer cells induced by TGF-beta 1. Indian J Pharm Educ Res2016; 50:583–590. DOI:10.5530/ijper.50.4.10

34-Yamamoto M, Suzuki A, Jokura H, Yamamoto N, Hase T. Glucosyl hesperidin prevents endothelial dysfunction and oxidative stress in spontaneously hypertensive rats. Nutrition2008; 24:470–476. DOI: 10.1016/j.nut.2008.01.010

To Cite:

Mahmoud, A., Mostafa, S., Hassan, E. The Possible Role of Hesperidin on Triolein Induced Lung Structural Changes in Adult Male Albino Rats (Histological and Immunohistochemical Study). ***Zagazig University Medical Journal*****, 2024; (1659-1670): -. doi: 10.21608/zumj.2024.292157.3411**